Enantioselective Ti(IV) Sulfoxidation Catalysts Bearing C_3-Symmetric Trialkanolamine Ligands: Solution Speciation by ^{1}H NMR and ESI-MS Analysis

Marcella Bonchio,[†] Giulia Licini,*,[†] Giorgio Modena,[†] Olga Bortolini,*,[‡] Stefano Moro,[§] and William A. Nugent[⊥]

Contribution from the Dipartimento di Chimica Organica, CMRO del CNR, via Marzolo 1, and Dipartimento di Chimica Farmaceutica, via Marzolo 9, Università di Padova, I-35131 Padova, Italy, Dipartimento di Chimica, via Borsari 46, Università di Ferrara, 44100 Ferrara, Italy, and The Du Pont Company, Central Research & Development, P.O. Box 80328, Wilmington, Delaware 19880-0328

Abstract: Sulfoxidation catalysts generated from titanium(IV) isopropoxide and enantiopure trialkanolamine ligands promote the enantioselective oxidation of aryl alkyl sulfides to the corresponding sulfoxides even at low (1−2%) catalyst loadings. Electrospray ionization mass spectrometry (ESI-MS), in combination with conventional low-temperature NMR techniques, provides a powerful tool for understanding the unique nature of these catalysts. Tetradentate ligation of the titanium atom by the trialkanolamine ligand provides a highly robust titanatrane core which is retained even in hydroxylic solvents and/or under acidic conditions. In contrast, the remaining apical coordination site is shown to be substitutionally labile. Previously ill-defined species formed when the catalyst is generated in situ with a slight excess of trialkanolamine are shown to consist of discrete 2:1, 3:2, and 4:3 oligomers in which the excess trialkanolamine bridges multiple titanatrane units. In the presence of excess *tert*-butyl hydroperoxide, all of the precatalyst species are cleanly converted to a mononuclear titanium(IV) peroxo complex which serves as the active sulfoxidation catalyst. Ab initio molecular orbital calculations were used to probe the structure and position of protonation of the catalytic species. Other ionization techniques (fast ion bombardment or electron impact) proved less useful than ESI-MS due to high levels of fragmentation during the ionization process.

Introduction

Central to the field of homogeneous asymmetric catalysis is the discovery of new transition-metal-based systems that are able to mediate organic reactions with high efficiency and selectivity.[1−3] Toward this end, an intensive research effort has been focused on the engineering of suitable chiral ligands[4,5] and on the study of their interactions with selected metal nuclei. The ultimate goal is the solution-phase production of a stable, kinetically competent, and highly stereoselective catalyst.[1−5] A rational approach toward this objective requires delineation of the key elements that are involved in such catalyst assembly, namely, the chiral ligand or its components, the achiral metal precursor, and any other additive eventually present in the reaction mixture.[1−6]

As far as oxygen-transfer catalysis is concerned, the Sharpless−Katsuki epoxidation system[7,8] launched the rich field of titanium-mediated asymmetric oxidations.[7−18] Since that breakthrough, chiral Ti(IV) alkoxides have been used to catalyze a variety of oxidative transformations, affording highly stereoselective processes in the allylic alcohol epoxidation,[7,8] β-hydroxyamine *N*-oxidation,[9] and sulfoxidation,[10−17] as well as the Baeyer−Villiger oxidation of cyclobutanones.[18] The general reaction protocol employs the achiral precursor titanium tetra-

---

* To whom correspondence should be addressed.

† Dipartimento di Chimica Organica, Università di Padova.

‡ Università di Ferrara.

§ Dipartimento di Chimica Farmaceutica, Università di Padova.

⊥ The DuPont Company.

(1) Ojima, I. *Catalytic Asymmetric Synthesis*; VCH Publisher: New York, 1993.

(2) Noyori, R. *Asymmetric Catalysis in Organic Synthesis*; Wiley-Interscience: New York, 1994.

(3) Nugent, W. A.; RajanBabu, T. V.; Burk, M. *Science* **1993**, *259*, 479−483.

(4) Seyden-Penne, J. *Chiral Auxiliaries and Ligands in Asymmetric Synthesis*; John Wiley & Sons: New York, 1995.

(5) Brunner, H.; Zettlmeier, W. *Handbook of Enantioselective Catalysts with Transition Metal Compounds*; VCH: Weinheim, 1993.

(6) Consider, for example, the detailed study on osmium(VIII)-mediated stereoselective dihydroxylation: Kolb, H. C.; VanNieuwenhze, M. S.; Sharpless, K. B. *Chem. Rev.* **1994**, *94*, 2483.

(7) Katsuki, T.; Sharpless, K. B. *J. Am. Chem. Soc.* **1980**, *102*, 5974.

(8) Gao, Y.; Hanson, R. M.; Klunder, J. M.; Ko, S. Y.; Masamune, H.; Sharpless, K. B. *J. Am. Chem. Soc.* **1987**, *109*, 5765.

(9) Miyano, S.; Lu, L. D.-L.; Viti, S. M.; Sharpless, K. B. *J. Org. Chem.* **1983**, *48*, 3608.

(10) Modena, G.; Furia, F. D.; Seraglia, R. *Synthesis* **1984**, 325.

(11) Pitchen, P.; Dunach, E.; Deshmuck, M. N.; Kagan, H. B. *J. Am. Chem. Soc.* **1984**, *106*, 8188.

(12) Brunel, J.-M.; Kagan, H. B. *Synlett* **1996**, 404.

(13) Komatsu, N.; Hashizume, M.; Sugita, T.; Uemura, S. *J. Org. Chem.* **1993**, *58*, 4529.

(14) Reetz, M. T.; Merk, C.; Naberfeld, G.; Rudolph, J.; Griebenow, N.; Goddard, R. *Tetrahedron Lett.* **1997**, *38*, 5273.

(15) Watson, K. G.; Fung, Y. M.; Gredley, M.; Bird, G. J.; Jackson, W. R.; Gountzos, H.; Matthews, B. R. *J. Chem. Soc., Chem. Commun.* **1990**, 1018.

(16) Superchi, S.; Rosini, C. *Tetrahedron: Asymmetry* **1997**, *8*, 349.

(17) Yamanoi, Y.; Imamoto, T. *J. Org. Chem.* **1997**, *62*, 8560.

(18) Lopp, M.; Payn, A.; Kanger, T.; Pehk, T. *Tetrahedron Lett.* **1996**, *37*, 7583.

isopropoxide [Ti(O-*i*-Pr)$_4$] in the presence of an enantiopure C_2-symmetric diol[19] and an alkyl hydroperoxide as the primary oxidant. Under such conditions, ligand exchange occurs in the coordination sphere of the titanium nucleus,[20,21] producing, among all the possible complexes, a chiral, highly reactive species (ligand-accelerating effect) which is responsible for the enantioselective outcome of the process.[22]

Due to the tendency of the Ti(IV) alkoxides to form mixtures of oligomeric complexes equilibrating in solution and because of the rapid ligand exchange equilibria,[22−24] for the majority of the processes cited above, the actual catalyst structure remains elusive. In all cases, a chiral, metal-centered η^2-peroxo species has been postulated as the reactive intermediate.[21] This latter hypothesis has been recently substantiated by the solid-state structure of the achiral η^2 *tert*-butylperoxotitanatrane dimer, which is, so far, the only reported X-ray structure of Ti(IV) alkylperoxo complex.[25] Despite the general lack of structural information, the majority of evidence collected in the literature for the different Ti(IV)/C_2-symmetric diol systems seems to agree about the aggregate nature of the enantioselective oxidant formed in solution.[11,13,20] As a matter of fact, in some protocols a supplementary dose of hydroxyl functionalities in the form of water or aliphatic alcohols is added to the reaction mixture to promote the assembly of oligomeric complexes, which are then much better catalysts than the precursors.[11−14]

Following the above discussion, it is possible to highlight the weak points affecting the Ti(IV)-based systems described thus far:

(1) The solution integrity of the active catalyst, likely oligomeric, is seriously jeopardized under turnover conditions by the excess of the hydroperoxide that, acting as a bidentate ligand toward the titanium center, can alter the nuclearity and/or substitute the chiral ligand in the coordination sphere of the metal.[24] Consequently, only ca. 20 catalytic cycles can be achieved without depletion of the system enantioselectivity.[8,12]

(2) The lack of information about the actual structure of the reactive titanium species hampers both rational catalyst engineering and detailed mechanistic studies.[20,21]

We have reported that a novel series of tetradentate alkoxide ligands, namely C_3-symmetric enantiopure trialkanolmines **1**, provide very stable titanium(IV) complexes.[24,26] In the presence of alkyl hydroperoxides, such species are able to mediate the asymmetric sulfoxidation of alkyl aryl sulfides with ee's up to 84% and with unprecedented catalytic efficiency, reaching 50−100 turnover numbers (Scheme 1).[26]

In this work we present a detailed study focused on (i) the structural evaluation of the catalytic Ti(IV)/**1** complexes, (ii) the establishment of their solution integrity both in the absence of the hydroperoxide and under catalytic conditions, and (iii) the direct observation of the *monomeric* reactive peroxometal complex involved in the enantioselective sulfoxidation.

(19) Derivatives of tartaric acid were employed in refs 7−12 and 18, 1,1′-binaphthol and its derivatives in refs 13 and 14, and 1,2-diaryl and di-*tert*-butylethane-1,2-diols in refs 15−17.

(20) Woodward, S. S.; Finn, M. G.; Sharpless, K. B. *J. Am. Chem. Soc.* **1991**, *113*, 106.

(21) Johnson, R. A.; Sharpless, K. B. In ref 1a, Chapter 4.1, pp 103−158.

(22) Berrisford, D. J.; Bolm, C.; Sharpless, K. B. *Angew. Chem., Int. Ed. Engl.* **1995**, *34*, 1059−1070.
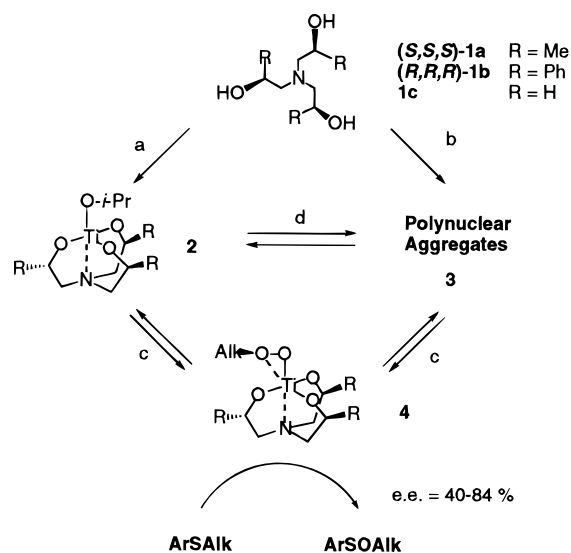
(23) Bradley, D. C.; Mehrota, R. C.; Gaur, D. P. *Metal Alkoxides*; Academic Press: London, 1978.

(24) Nugent, W. A.; Harlow, R. L. *J. Am. Chem. Soc.* **1994**, *116*, 6142 and references therein.

(25) Boche, G.; Möbus, K.; Harms, K.; Marsh, M. *J. Am. Chem. Soc.* **1996**, *118*, 2770.

(26) Di Furia, F.; Licini, G.; Modena, G.; Motterle, R.; Nugent, W. A. *J. Org. Chem.* **1996**, *61*, 5175.

Scheme 1[a]

[a] Reagents and conditions: (a) stoichiometric Ti(*i*-PrO)$_4$, CHCl$_3$, 20 °C; (b) Ti(*i*-PrO)$_4$ (0.75 equiv), CH$_2$Cl$_2$, 20 °C, followed by solvent removal; (c) alkyl hydroperoxide; (d) excess of **1**.

Our approach employs electrospray ionization mass spectrometry (ESI-MS),[27] combined with standard ^{1}H NMR analysis, to assess the nature of the various titanium species equilibrating in solution under different reaction conditions and their evolution to the active species originating by interaction with *tert*-butyl hydroperoxide (TBHP). From the results obtained, structures of the key Ti(IV) complexes are proposed and discussed by comparison with experiments performed using different ionization techniques: fast ion bombardment (FIB$^+$) and electron impact (EI) and ab initio calculations.

Results and Discussion

Ligands **1** bind tightly to the titanium center in a tetradentate fashion, producing complexes whose nature depends on the stoichiometry of the reaction with Ti(O-*i*-Pr)$_4$ (Scheme 1).[24,26,28]

When a precise 1:1 ligand/Ti(IV) ratio is employed, catalyst **2** is obtained (Scheme 1, path a), whose spectroscopic behavior is consistent with a monomeric structure. In contrast, a complex mixture of polynuclear Ti(IV)-based species **3** forms from the interaction of Ti(IV) with a slight excess of ligand **1** (Scheme 1, path b). Upon removal of the solvent containing the 2-propanol released in the reaction, catalyst **3** is isolated as a white powder and is routinely used to mediate asymmetric sulfoxidation.[26] In fact, it provides faster reaction rates than the in situ-formed system **2**, where the liberated 2-propanol behaves as a competing ligand. Furthermore, it offers a practical advantage in handling.

The room-temperature ^{1}H NMR spectrum of **3** shows broad resonances, indicating the presence of a mixture of slowly equilibrating aggregates. In a recent communication, we have shown that the characterization of the diverse species present in **3** can been achieved through ESI-MS and ^{1}H NMR analysis.[28] Here we report the complete study that has been performed both on the in situ-formed species **2** and on the isolated catalyst **3**. Our results also include the investigation of such systems in the presence of TBHP, which reacts with **2** and **3**, yielding the same monomeric Ti(IV) peroxo species **4** (Scheme 1, path c).

(27) Colton, R.; D'Agostino, A.; Traeger, J. C. *Mass Spectrom. Rev.* **1995**, *14*, 79 and references therein.

(28) Bonchio, M.; Licini, G.; Modena, G.; Moro, S.; Bortolini, O.; Traldi, P.; Nugent, W. A. *Chem. Commun.* **1997**, 869.
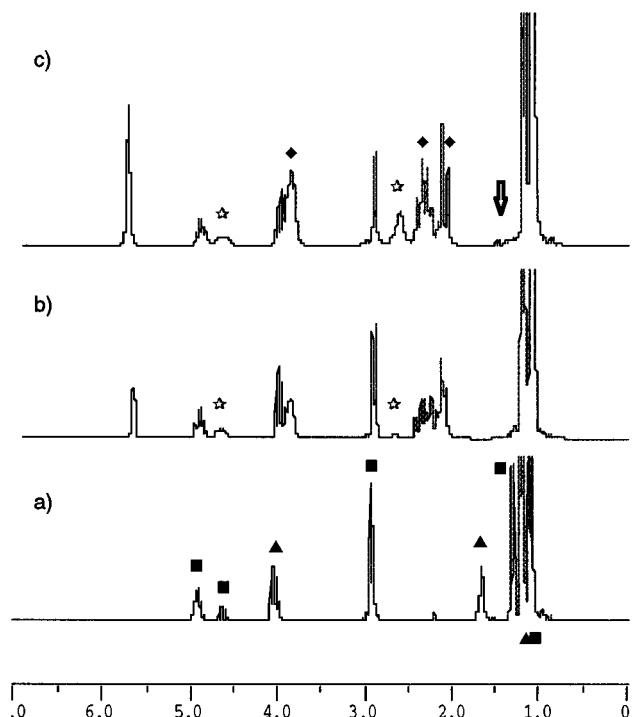
Figure 1. ^{1}H NMR titration of in situ-formed complex **2a** (2.5×10^{-2} M) by **1a** in deuteriochloroform at -10 °C for Ti(IV): **1a** ratios (a) 1:1, (b) 1:3, and (c) 1:5. Resonances are relative to (■) complex **2a**, (▲) displaced 2-propanol, (◆) ligand **1a**, and (☆) newly formed titanium species (see discussion in the text and eq 1).

The collected ESI-MS spectra, together with tandem MS^n analysis and the simulation of the observed isotopic distributions, have provided clear insight in the structural elucidation of the Ti(IV) complexes under study. There are precedents in the literature where ESI-MS has been applied successfully to the identification of different polynuclear metal complexes and has proved to be an effective tool for the investigation of rapid exchanging systems.[27,29] In this study, ESI-MS has emerged as a diagnostic technique which provides a powerful alternative to low-temperature NMR spectroscopy.

Ti(IV)/1a in Situ-Formed System: Catalyst 2a. System **2a** is prepared in situ by reacting stoichiometric amounts of (*S,S,S*)-tri-2-propanolamine **1a** with Ti(*i*-PrO)$_4$. Its ^{1}H NMR spectrum at -10 °C[30] (Figure 1, spectrum a) in deuteriochloroform shows a single set of signals at $\delta = 1.10$, 2.80−2.95, and 4.80−4.98 ppm respectively for the methyl, methylene, and methine groups of coordinated **1a**. Signals corresponding to the two diastereomeric methyl groups and to the methine of the bonded isopropoxy ligand can be observed at $\delta = 1.31$ (CH$_3$) and 4.62 ppm (CH). According to the stoichiometry of the equilibrium, favoring the formation of the chelated complex **2a**, 3 equiv of *i*-PrOH are displaced in solution [$\delta = 1.20$ (CH$_3$) and 4.01 ppm (CH)].

The ^{1}H NMR data are consistent with a solution-phase monomeric structure for complex **2a**. Addition of increasing amounts of ligand **1a** to the system (Figure 1, spectra b and c) causes the disappearance of the apical isopropoxy ligand resonances and the synchronous appearance of two broader signals at $\delta = 2.7$ and 4.6−4.8 ppm. It is noteworthy that the

(29) Løver, T.; Henderson, W.; Bowmaker, G. A.; Seakins, J. M.; Cooney, R. P. *Inorg. Chem.* **1997**, *36*, 3711 and references therein.

(30) ^{1}H NMR spectra have been recorded at low temperature in order to shift the resonance of the free hydroxy group in a region far away from the signals of interest. At -10 °C, it was observed at 1.65 ppm (see Figure 1, spectrum a).

latter resonance has the same chemical shift found for the methine of the isopropoxide ligand.

Considering the similar structure of the two competing alkoxides (Me$_2$CHO− and R$_2$NCH$_2$CHMeO−), this result suggests that these new signals can be assigned to the methine and methylene protons of one arm of ligand **1a** that has displaced the apical isopropoxy ligand in **2a**. Such a modification of the coordination sphere of the titanium nucleus does not influence the local C_3 symmetry of the chelated titanatrane moiety, whose resonances remain basically unchanged. Therefore, the new Ti(IV) species displays two molecules of **1a** in its coordination sphere with a diverse spatial arrangement. However, the integration of the signals assigned to the different protons of the coordinated ligands, namely the one involved in the chelated atrane structure and the other in the apical position, does not provide significative evidence for the straightforward assignment of the structure of the new complex. Signals corresponding to the nonligated trialkanolamine **1a** are at $\delta = 3.8$−4.0 (CH), 2.37 and 2.19 (CH$_2$), and 1.20 ppm (CH$_3$).

On the basis of the NMR evidence reported above, eq 1 can be put forward to describe the equilibria occurring in solution. Likely, the polyalcoholic nature of the ligand can promote the formation of Ti(IV)-based oligomers. As a matter of fact, a total of 5 equiv of ligand **1a** versus Ti(O-*i*-Pr)$_4$ (Figure 1, spectrum c) causes the total displacement of the apical isopropoxy ligand.

(eq. 1)
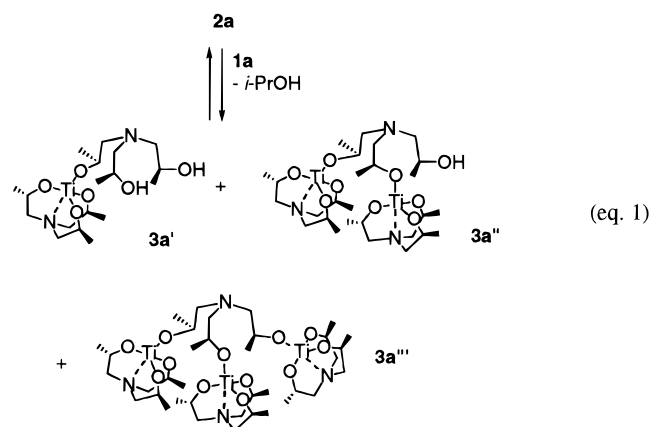
The presence of polynuclear aggregates **3a′**, **3a″**, and **3a‴** has been unequivocally confirmed by positive ion ESI mass spectrometry (Chart 1 and Figure 2).
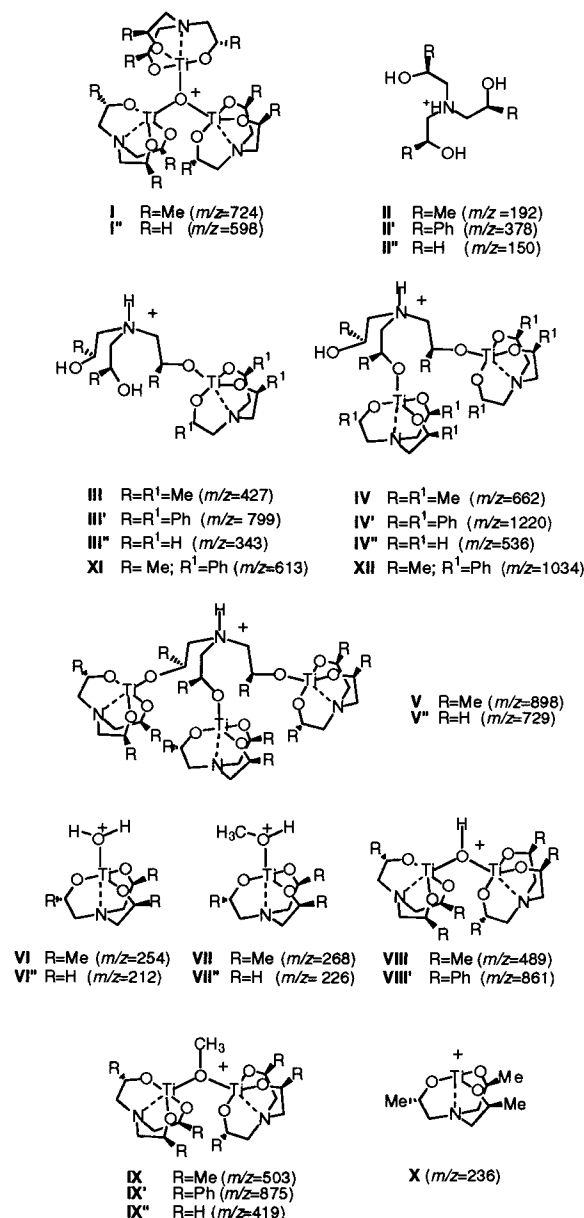
The ESI-MS experiments were conducted to investigate the nature of the titanium complexes originating when an acidic chloroform solution[31] of Ti(O-*i*-Pr)$_4$ is "titrated" with progressive additions of the chiral ligand **1a** (Figure 2). The positive ion spectrum collected for the 1:1 system shows a single intense peak at $m/z = 724$ (**I**) (Figure 2, spectrum a). As the molecular ion peak corresponding to the protonated monomeric complex **2a** would be expected at $m/z = 295$, this observation stands in contrast with the previously discussed ^{1}H NMR analysis (see Figure 1, spectrum a). Indeed, the experimental cluster ion peaks of ion **I** (see Experimental Section) correspond to a trinuclear titanium species, namely [TiN(CH$_2$CHMeO)$_3$]$_3$O$^+$. Although the molecular composition of ion **I** retains the correct 1:1 stoichiometry, as established between Ti(IV) and ligand **1a** in the initial experimental conditions, the lack of the isopropoxy residues and its aggregate nature indicate that the transfer of complex

(31) Stock solutions of chloroform (stabilized with silver foils) were routinely used with no acidic additives.

Chart 1

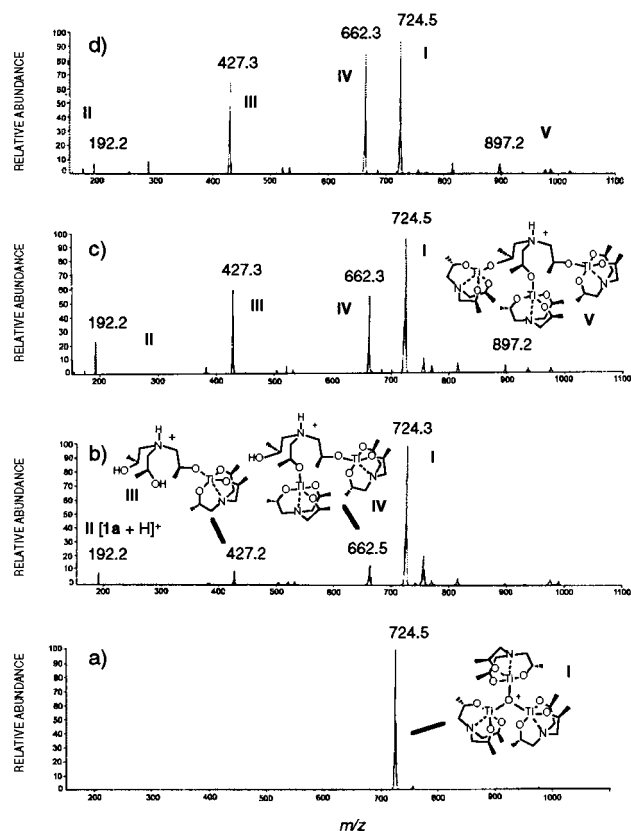**Figure 2.** ESI-MS titration of in situ-formed complex **2a** (2.5×10^{-3} M) by **1a** in acidic chloroform as mobile phase for Ti(IV): **1a** ratios (a) 1:1, (b) 1:3, (c) 1:5, and (d) 1:7.

Table 1. MS^2 Fragment Ions after Collision-Induced Dissociation of Ions **I** ($m/z = 724$), **II** ($m/z = 192$), **III** ($m/z = 427$), **IV** ($m/z = 662$), and **V** ($m/z = 897$)[33]
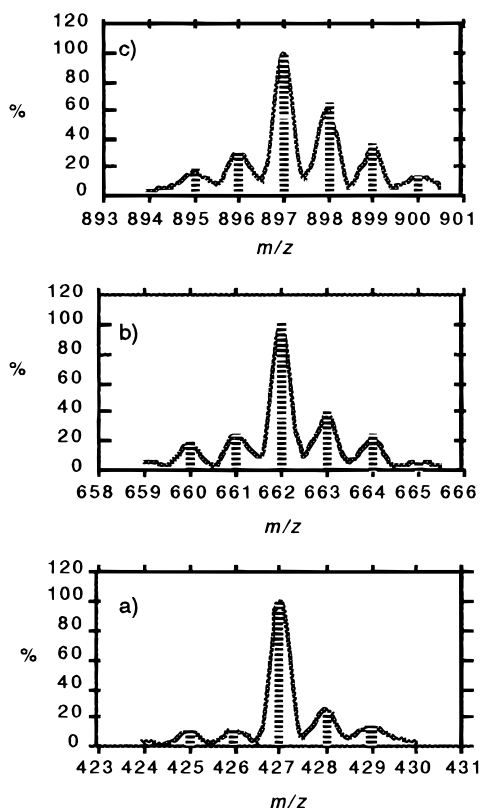
ion	principal ions,[a] m/z (relative intensity)	identification
I	724 (10)	M$^+$
	680 (100)	M$^+$ − MeCHO
	636 (6)	M$^+$ − 2MeCHO
II	192 (2)	[M + H]$^+$
	174 (100)	[M + H − H$_2$O]$^+$
	156 (13)	[M + H − 2H$_2$O]$^+$
	138 (2)	[M + H − 3H$_2$O]$^+$
III	427 (3)	[M + H]$^+$
	409 (16)	[M + H − H$_2$O]$^+$
	294 (16)	[M + H − C$_6$H$_{15}$NO$_2$]$^+$
	174 (100)	[**1a** + H − H$_2$O]$^+$
IV	662 (29)	[M + H]$^+$
	644 (5)	[M + H − H$_2$O]$^+$
	489 (14)	[M + H − **1a** + H$_2$O]$^{+b}$
	409 (100)	[M − TiN(CH$_2$CHMeO)$_3$ − H$_2$O]$^+$
V	897 (8)	[M + H]$^+$
	644 (18)	[M + H − TiN(CH$_2$CHMeO)$_3$ − HO]$^+$
	409 (100)	[M + H − 2TiN(CH$_2$CHMeO)$_3$ − O]$^+$

^{a} Ions are identified by the peak of great intensity in the isotope distribution pattern. ^{b} Ion likely originating from the reaction of fragment [M + H − **1a**]$^+$ with water molecules present in the ion trap (ref 33).

2a from solution into the gas phase occurs with decomposition and produces a major reorganization of the metal species.[32]

Tandem MS^2 analysis (Table 1) shows that ion **I** fragments by losing one and two acetaldehyde molecules. Such a fragmentation pattern is strong evidence for the coordination of ligand **1a** to the titanium nucleus. In fact, the MS^2 spectrum of ion **II** ($m/z = 192$) collected for a chloroform solution of **1a** under identical experimental conditions and corresponding to the protonated trialkanolamine **1a** produces only fragments resulting from the loss of one, two, or three molecule of water (see Table 1). This observation suggests that the chelated titanatrane structure retains its integrity during the electrospray process and that oxonium ion **I** likely originates from the loss of the more labile apical isopropoxy ligand. Following this decomposition process, yielding the highly reactive cationic species [TiN(CH$_2$CHMeO)$_3$]$^+$ (vide infra), reaction with traces of water present in the mobile phase could eventually lead to the formation of ion **I**. Indeed, the isotopic cluster of ion **I** shows

^{18}O incorporation (65%) when H$_2$^{18}O is intentionally added to the mobile phase (see Experimenal Section).

The other experiments reported in Figure 2, spectra b−d, provide an unequivocal picture of the modifications occurring in the system under examination when an excess of **1a** with respect to the Ti(IV) precursor is added. In fact, notwithstanding the presence of ESI-induced reactions (in all the spectra, the base peak is still ion **I**), the progressive appearance of three

(32) Variation of the spray voltage (2−7 kV), of the capillary voltage (10−50 V), and of the temperature (80−180 °C) does not affect the speciation pattern in the in situ **2a** system.

Figure 3. Observed (—) and calculated (||||) isotope distribution patterns of ions (a) **III** ($m/z = 427$), (b) **IV** ($m/z = 662$), and (c) **V** ($m/z = 897$).

new titanium-based ions is monitored at $m/z = 427$ (**III**), 662 (**IV**), and 897 (**V**). Their composition corresponds respectively to the 2:1, 3:2, and 4:3 protonated adducts of ligand **1a** with the titanium nucleus, as revealed by the inspection of the experimental isotopic clusters (Figure 3). This observation confirms the solution-phase formation of titanium-based oligomers in line with the hypothesis of eq 1[34] and their capability to survive, at least in part, to the ESI ionization conditions.

Tandem MS[2] analysis provides a further characterization of species **III**, **IV**, and **V** (Table 1). The comparative analysis of their fragmentation patterns allows the recognition of a common cascade motif, thus indicating that ions **III**, **IV**, and **V** are homologues (Figure 4).

In particular, the higher aggregate, ion **V** ($m/z = 897$), containing three chiral titanatrane units, decays to species at $m/z = 644$ and 409 with respectively two and one titanium center. In a similar fashion, ion **IV** leads to the mononuclear titanium species at $m/z = 409$ that is also generated in the MS[2] spectrum of ion **III** (Table 1). Moreover, the isobaric ions at $m/z = 409$, originating from the collision-induced dissociation (CID) of the three precursors **III**, **IV**, and **V**, afford identical MS[3] spectra (Figure 4). On the basis of this evidence, we attribute the molecular ions under examination to the protonated species **3a′**, **3a″**, and **3a‴**, whose existence has been postulated according to eq 1.

Ti(IV)/1a Preformed System: Catalyst 3a. Compared with the monomeric system **2a**, the ^{1}H NMR of the preformed catalyst **3a** (Scheme 1, path b) shows a more complex system.

(33) A similar process has been reported for Pt(II) allylic compounds: Favaro, S.; Pandolfo, L.; Traldi, P. *Rapid Commun Mass Spectrom.* **1997**, *11*, 1859–1866.

(34) The location of the protonation site in ions **III**, **IV**, **V**, **XI**, and **XII** cannot be precisely assigned via ESI-MS. We will assume that the protonation occurs at the nitrogen atom of the apical trialkanolamine ligand.
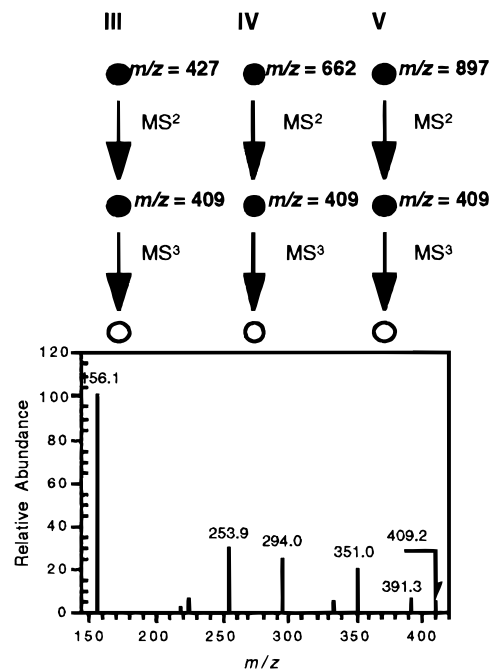
Figure 4. MS[2] fragment ions after collision-induced dissociation (CID) of the isobaric $m/z = 409$ peaks originating from the fragmentation of ions **III**, **IV**, and **V**.
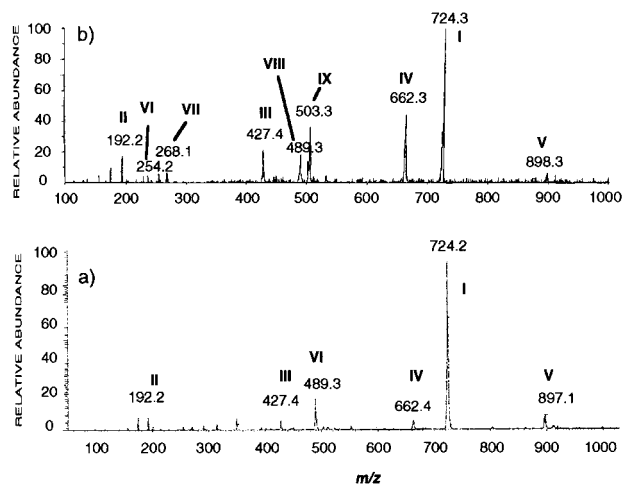
Figure 5. ESI-MS spectra of complex **3a** (2.5×10^{-3} M) in (a) acidic chloroform[31] and (b) methanol as mobile phases with peak assignments indicated.

No signals corresponding to the coordinated and free 2-propanol can be detected, and broader peaks relative to the chiral titanatrane unit can be recognized at $\delta = 4.93$ (CH), 2.80–2.98 (CH$_2$), and 1.08–1.21 ppm (CH$_3$). While ^{1}H NMR analysis confirms that the trialkanolamine **1a** is the only ligand present in the coordination sphere of the titanium(IV) nucleus, it does not provide direct evidence of the existence of species **3a′**, **3a″**, and **3a‴**.

Again, ESI-MS has proved to be a more diagnostic tool. The positive ion ESI-MS spectrum of **3a** has been collected in two different mobile phases, namely acidic chloroform[31] and methanol (Figure 5).

In both spectra, ions **III**, **IV**, and **V** are present, together with the oxonium complex **I** and the protonated free ligand **II**. When methanol is the mobile phase (Figure 4, spectrum b), additional peaks corresponding to other titanium complexes deriving from the interaction of **3a** with the solvent itself and water can be detected. Low-abundance ions at $m/z = 254$ (**VI**) and 268 (**VII**)

Table 2. FIB$^+$-MS and EI-MS Data for Complex **3a**

| principal ions,[a] m/z	indentification	FIB$^+$-MS[b] (%)	EI-MS (%)
192	**II**	94	17
236	**X**	100	48
280	[Ti(N(CH$_2$CHMeO)$_3$(MeCHO))]$^+$	nd[c]	35
294	[Ti(N(CH$_2$CHMeO)$_3$(CH$_2$CHMeO))]$^+$	nd	52
381	[Ti(N(CH$_2$CHMeO)$_3$N(CH$_2$CH-MeOH)$_2$(CH$_2$CHMeO))]$^+$	nd	22
389	**X** + NO$_2$C$_6$H$_4$CH$_2$OH	19	nd
427	**III**	20	nd
624	[(Ti(N(CH$_2$CHMeO)$_3$))$_2$OCH-C$_6$H$_4$NO$_2$]$^+$	22	nd
724	**I**	30	nd

[a] Ions are identified by the peak of great intensity in the isotope distribution pattern. [b] 3-nitrobenzyl alcohol as matrix. [c] Not determined.

can be assigned to the mononuclear chiral titanatrane moiety bearing an axial molecule respectively of water or methanol. Ions at $m/z = 489$ (**VIII**) and 503 (**IX**) show an isotopic distribution and tandem MS^2 spectra (see Experimental Section), consistent with binuclear structures containing a hydroxy and methoxy residue, likely bridging between two titanium nuclei. Isotopic labeling experiments performed with perdeuteriomethanol further confirm the assignment of ion **IX**[28] (see Experimental Section). It is important to notice that, despite the strongly competing solvent, the chelated titanatrane complexes are reasonably stable and can be detected in spectrum b (Figure 5).

MS spectra of **3a** have also been obtained using different ionization techniques. Data reported in Table 2 allow the comparison of the results obtained under fast ion bombardment (FIB$^+$) and electron impact (EI) ionization conditions.

Although the FIB$^+$-MS technique has been used in solution-phase complexation studies to assess the correspondence between solution- and gas-phase phenomena, in the case of the titanium catalyst under examination it does not provide a straightforward answer. The problem affecting the FIB$^+$-MS experiment is twofold. First, there are ions produced from the reaction of the titanium catalyst with the 3-nitrobenzyl alcohol matrix or with the water present in it, i.e., species at $m/z = 624$ and 389, and the already discussed ion **I** ($m/z = 724$). Second, it shows a higher degree of fragmentation as compared with the ESI-MS results. This last conclusion originates from the observation that the base peak of the FIB$^+$-MS spectrum corresponds to ion **X** ($m/z = 236$), whose composition, supported by isotopic cluster and MS^2 analysis (see Experimental Section), can be ascribed to the cationic metal species [TiN(CH$_2$-CHMeO)$_3$]$^+$. Moreover, at higher mass-to-charge ratios, there is no trace of the oligomeric titanium-based ions **IV** and **V**, and the monomeric homologue **III** is detected only with low intensity ($\sim$20%). Major fragmentation is expected in the mass spectrum collected for **3a** in the EI ionization mode. Indeed, the only detected peaks occur in the monomeric region at $m/z = 381$ (Table 2), deriving from the breakdown of the apical trialkanolamine ligand with consequent destruction of the Ti(IV) oligomers. Moreover, also in the EI-MS spectrum, ion **X** is one of the dominant peaks.

The gas-phase production of a titanium-centered cation **X** bearing the polyfunctional ligand **1a** is of particular interest. In general, the study of transition-metal-containing ions offers the unique opportunity to investigate the "intrinsic" properties and reactivity of such species, in the absence of complicating effects such as solvation and counterion effect, and at the same time, it can provide important clues about their behavior in the
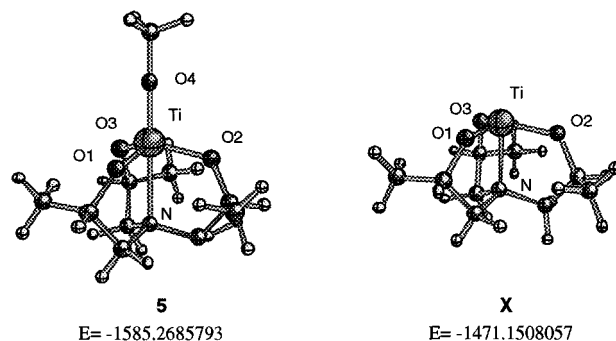
Figure 6. Ab initio [RHF/3-21G(*)] optimized structures and energies (Hartrees) of (*S,S,S*)-Ti[N(CH$_2$CHMeO)$_3$MeO) **5** and cationic species **X**.

Table 3. Selected Bond Distances (Å) and Atomic Charges for (*S,S,S*)-Ti(NCH$_2$CH$_2$O)$_3$(MeO) (**5**) and Cationic Species (*S,S,S*)-**X** Calculated at the RHF/3-21G(*) Theoretical Level

compound	distances (Å)	atomic charges
5	Ti−O(1) = 1.815	Ti = 1.53
	Ti−O(2) = 1.814	O(1) = −0.81
	Ti−O(3) = 1.815	O(2) = −0.82
	Ti−O(4) = 1.747	O(3) = −0.81
	Ti−N = 2.397	O(4) = −0.53
		N = 0.56
ion **X**	Ti−O(1) = 1.753	Ti = 2.10
	Ti−O(2) = 1.753	O(1) = −0.91
	Ti−O(3) = 1.753	O(2) = −0.91
	Ti−N = 2.142	O(3) = −0.91
		N = 0.37

condensed phase.[35] Significantly, ion **X** is generated only under FIB$^+$ and EI conditions, while in the ESI-MS experiments only its formal adducts with oxygenated ligands (water, methanol, and the trialkanolamine itself) are detected.

While the gas-phase reactivity of ion **X** with neutral oxygen donor ligands will be the object of a separate communication, in this paper we report the results of ab initio theoretical calculations, performed at the RHF/3-21G(*) level, to determine the geometries, energies, and atomic charge distributions of the neutral complex (*S,S,S*)-Ti[(MeO)N(CH$_2$CHMeO)$_3$] (**5**) and of the cationic species **X**. As shown in Figure 6 and Table 3, the high-energy cation **X** displays a compressed structure with shorter titanium−oxygen and titanium−nitrogen bonds. The positive charge is distributed on the entire molecule, as indicated by the variation of all atomic charges, with respect of the neutral species **5**. It is possible to conclude that the polydentate ligand **1a** has a stabilizing effect on the metal ion, which retains the tetracoordination around the Ti(IV) center and survives the conditions of the FIB$^+$ and EI experiments.
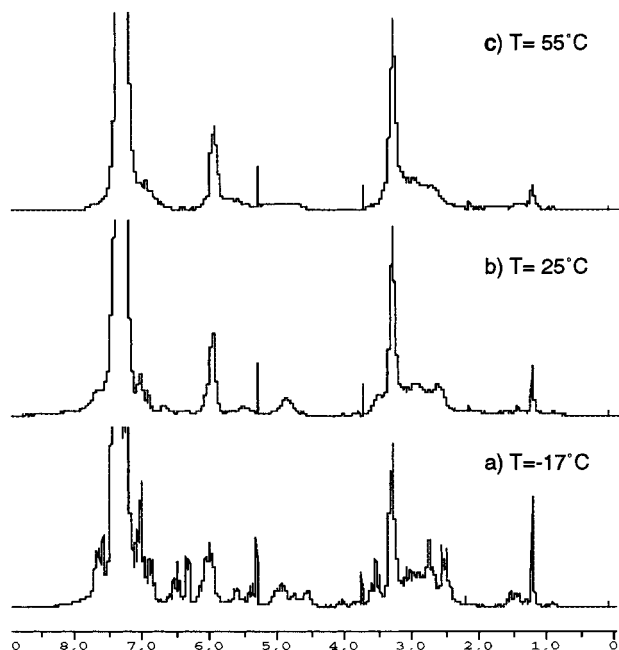
Ti(IV)/1b or 1c Preformed Systems: Catalysts 3b and 3c and Crossed -Type Complexes. The preformed Ti(IV) complexes with ligands **1b** and **1c** were prepared according to Scheme 1, path b, and examined by positive ESI-MS. Methanol solutions of species **3b** and **3c** show ESI-MS patterns in perfect analogy with the one described above for system **3a** (see Table 4).[28]

Therefore, a common feature of all isolated catalysts **3a**−**c** is that they consist of a mixture of oligomeric Ti(IV) complexes with similar structure. It should be pointed out that, among the catalysts examined, **3b** affords the most enantioselective sulfoxidation system, whose merits are mentioned in the Introduction. In this light, its solution-phase composition has been further

(35) Frieser, B. S. *Acc. Chem. Res.* **1994**, *27*, 353−360.

6264   *J. Am. Chem. Soc., Vol. 121, No. 26, 1999*

Bonchio et al.

Table 4. ESI-MS Data for Complexes **3b** and **3c** (2.5×10^{-3} M, Methanol)[a]

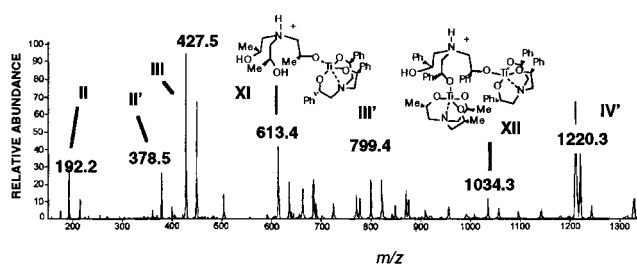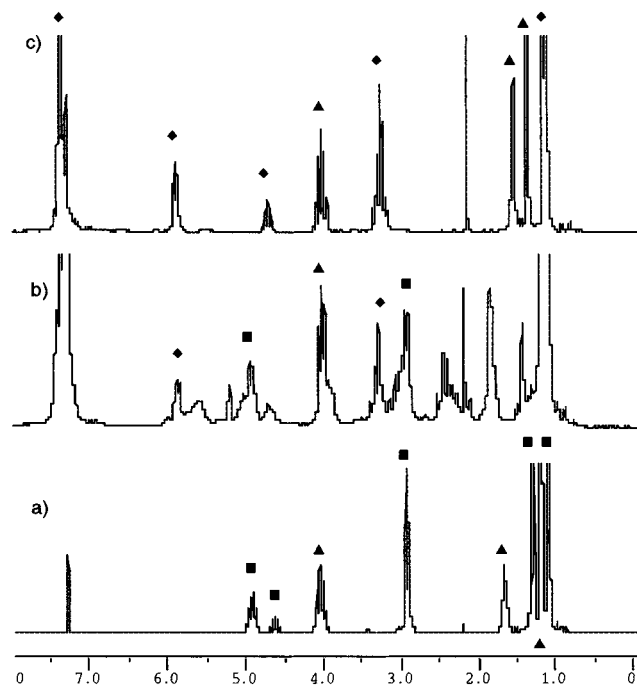| system	ion[a]	m/z	system	ion[a]	m/z
4b	**I′**	nd[a,b]	**4c**	**I″**	598
	II′	378		**II″**	150
	III′	799		**III″**	343
	IV′	1220		**IV″**	536
	V′	nd[b]		**V″**	729
	VI′	nd		**VI″**	212
	VII′	454		**VII″**	226
	VIII′	861		**VIII″**	nd
	IX′	875		**IX″**	419

[a] Ions are identified by the peak of great intensity in the isotope distribution pattern. [b] "nd" indicates m/z values over instrument detection limit.


Figure 8. ESI-MS spectrum in methanol of **3a** (2.5×10^{-3} M) upon addition of a large excess of **1b**, with peak assignments indicated. In ions **XI** (m/z = 613) and **XII** (m/z = 1034), the relative position of ligands **1a** and **1b** in the coordination sphere of Ti(IV) is arbitrary.

Figure 7. Temperature-dependent ^{1}H NMR spectra of complex **3b** (2.5×10^{-2} M) in deuteriochloroform at (a) − 17, (b) 25, and (c) 55 °C.

Figure 9. ^{1}H NMR spectra in deuteriochloroform at −10 °C of (a) complex **2a** (2.5×10^{-2} M), (b) complex **2a** (2.5×10^{-2} M) + **1b** (2.5×10^{-2} M), and (c) complex **2b** (2.5×10^{-2} M). Resonances are relative to (■) complex **2a**, (◆) complex **2b**, and (▲) displaced 2-propanol. The other resonances are relative to the free ligands **1a** and **1b**.

investigated through ^{1}H NMR at variable temperatures (Figure 7).[28]

The spectral changes, observed within the range from −17 to +55 °C for a deuteriochloroform solution of **3b**, definitely indicate the presence of Ti(IV)-based polynuclear complexes equilibrating in solution. Specifically, while at high temperature only three broad signals are detected (Figure 7, spectrum c), each one corresponding to the different type of protons present in ligand **1b** (CH, CH$_2$, and C$_6$H$_5$), at lower temperature the system freezes out (Figure 7, spectrum a), yielding a major number of resonances with different intensities and spanning a wide range of frequencies. The latter observation is consistent with the existence in solution of stable nonsymmetric aggregates, thus supporting the ESI-MS results.

Further evidence both on the nature of oligomers **3** and on the occurrence of ligand-exchange equilibria affecting their solution integrity has been achieved by ESI-MS and ^{1}H NMR analysis of system **3a** in the presence of ligand **1b** as additive. The experiments have been designed to monitor the presence of crossed-type Ti(IV)/**1a**,**b** complexes eventually formed through ligand scrambling. Following this idea, the ESI-MS spectrum of system **3a** has been collected under the same conditions of the Figure 5b experiment, but adding an excess of ligand **1b** to the mobile phase. New peaks arising at m/z =

613 (**XI**) and 1034 (**XII**) are, indeed, observed whose composition reveals the simultaneous coordination of both ligands **1a** and **1b** to the Ti(IV) center (Figure 8).

The proposed assignment of their structures is indicated directly on the spectrum (Figure 7) and follows the straightforward analogy with species **3′** and **3″**. Moreover, ions at m/z = 799 (**III′**) and 1220 (**IV′**) (see also Table 4) indicate the presence of complexes where the original ligand **1a** has been completely substituted by **1b** in the coordination to the titanium(IV) nucleus.

Direct proof of ligand scrambling occurring in solution is also provided by the modification of the ^{1}H NMR spectrum of the in situ-formed catalyst **2a** upon addition of 1 equiv of ligand **1b.** In Figure 9, spectra a and c allow the identification of the resonances pertaining to the single monomeric catalysts **2a** and **2b** and their comparison with the mixed system **2a** + **1b** (Figure 9, spectrum b).[36] In the latter spectrum, the simultaneous

(36) An analogous result can be obtained if a different addition order of the reagents is used, namely by adding Ti(*i*-PrO)$_4$ to equimolar amounts of premixed ligands **1a** and **1b** (see ^{1}H NMR spectra reported in Figure 1S, Supporting Information).
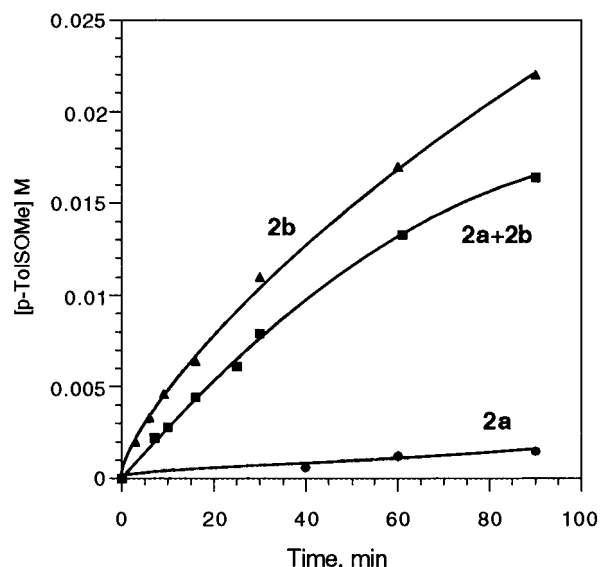
Figure 10. Plot of benzyl *p*-tolyl sulfoxide formation vs time (min) in the oxidation of benzyl *p*-tolyl sulfide (0.27 M) by CHP (0.027 M) in DCE at −20 °C, catalyzed by (●) **2a**, (▲) **2b**, and (■) **2a** + **2b** (for experimental conditions, see footnote to Table 5).

Table 5. Stereoselective Sulfoxidation of Benzyl *p*-Tolyl Sulfide (0.27 M) by CHP (0.027 M) Catalyzed by in Situ-Formed Systems **2a**, **2b**, and **2a** + **2b** in DCE at −20 °C[a]

entry	system	ligand $\times 10^3$ (M)	k_{obs} $\times 10^4$ (s^{-1})	ee (%) (absolute configuration)
1	(*S,S,S*)-**2a**	**1a** (3.6)	0.12 ± 0.014	12 (*R*)
2	(*R,R,R*)-**2b**	**1b** (3.6)	2.51 ± 0.13	53 (*S*)
3	(*S,S,S*)-**2a** + (*R,R,R*)-**2b**	**1a** (1.8) + **1b** (1.8)	1.57	52 (*S*)

[a] In all the reactions, [Ti(*i*-PrO)₄] = 3.3 × 10⁻³ M, and ligand **1** according to the table.

appearance of signals corresponding to the chiral titanatrane moiety with chelated **1b** and to the displaced ligand **1a** is observed, thus indicating the coexistence in solution of both catalytically active complexes **2a** and **2b**.

In this respect, a key observation is provided by the examination of the asymmetric oxidation of benzyl *p*-tolyl sulfide with cumyl hydroperoxide (CHP) in the presence of the different catalytic systems. The aim of such investigation is to test the single catalysts **2a** and **2b** and the mixed system (Ti(*i*-PrO)₄ + **1a** + **1b**) under the twofold profile of reaction kinetics and enantioselectivity (Figure 10 and Table 5).

Inspection of the pseudo-first-order rate constant (k_{obs}) values reported in Table 5 reveals that (i) catalysis by **2a** is negligible with respect to **2b**, whose reactivity is superior by 1 order of magnitude (cf. entries 1 and 2 in Table 5) and (ii) in the mixed system, where **2a**:**2b** ≈ 50:50, the two catalysts behave independently, displaying a "solo" reactivity, and their contribution to the overall reaction rate is additive, so that a predictable reduction of the rate constant to one-half is, indeed, observed (cf. entries 2 and 3 in Table 5). As a consequence of the ligand-accelerating effect,[22] induced by the chiral trialkanolamine **1b**, the enantiomeric excess of the sulfoxide recovered either in the reaction catalyzed by **2b** alone or by the mixed system (**2a** + **2b**) is basically the same (cf. entries 2 and 3 in Table 5). The above observations are unanimous in support of the independent reactivity of the two enantiopure catalysts produced in solution through ligand exchange equilibria involving **1a**, **1b**, and the achiral precursor Ti(O-*i*-Pr)₄; moreover, they raise the issue of

Table 6. ¹H NMR Spectral Data for *tert*-Butyl Peroxo Complexes **4a**−**c** in Deuterochloroform at 21 °C

compd	¹H NMR (δ, ppm)[a]
4a	1.09 (d, *J* = 6.0 Hz, 9H), 1.47 (s, 9H), 2.95−3.03 (AB system, 6H), 4.91−5.08 (m, 3H)
4b	1.58 (s, 9H), 3.32 (dd, *J* = 11.9, 4.4 Hz, 3H);, 3.43 (dd, *J* = 11.9, 10.6 Hz, 3H), 5.98 (dd, *J* = 10.6, 4.4 Hz, 3H), 7.20−7.48 (m, 15H)
4c	1.48 (s, 9H), 3.26 (t, *J* = 6.0 Hz, 6H), 4.50 (t, *J* = 6.0 Hz, 6H)

[a] Relative to TMS.

the nature of the active peroxometal complex generated under the conditions of catalytic sulfoxidation, which will be addressed in the next paragraph.

Ti(IV)/1 Alkyl Hydroperoxides. As already mentioned in the Introduction, titanium η^2-alkyl peroxo complexes are considered the active oxidants in the catalytic cycle employing Ti(IV) alkoxide precursors and alkyl hydroperoxides as oxygen donors[20,21] (Scheme 1). Direct evidence of the existence of such reactive intermediates is provided by the solid-state structure of η^2-*tert*-butyl peroxotitanatrane dimer which is, so far, the only characterized Ti(IV) peroxo complex.[25] However, X-ray data may be of limited utility or even misleading for the assignment of the solution-phase structure of complexes that exchange ligands as readily as titanium(IV) alkoxides do. In the case of the Ti(IV)/**1** systems, ¹H NMR allows the monitoring of the formation of the peroxidic species **4** when an excess of *tert*-butyl hydroperoxide (TBHP) is added to catalysts **2** or **3** (Scheme 1, path c). In particular, under catalytic conditions, e.g., in the presence of an excess of the primary oxidant TBHP, both the monomeric system **2** and the oligomeric complexes **3** *quantitatively* evolve to species **4**. The ¹H NMR resonances pertaining to **4** are those of a highly symmetric Ti(IV) species. In fact, a single set of signals is observed for each type of protons of the chiral titanatrane unit, and a singlet is observed corresponding to the coordinated *tert*-butylperoxo group (Table 6).

The spectroscopic evidence points to a monomeric structure for the peroxotitanium species formed in solution under catalysis conditions.[37] Additional support for a monomeric structure comes from the characterization via ESI-MS of the protonated Ti(IV) peroxo complexes **4a** (*m/z* = 326, ion **XIII**) and **4c** (*m/z* = 284, ion **XIII″**), whose formation is monitored upon addition of TBHP to the mobile phase (methanol or acidic chloroform) containing **3a** or **3c**. Analysis of the isotopic clusters[28] and MS² studies (see Experimental Section) of both ions **XIII** and **XIII″** provides direct proof of the monomeric structure of peroxo complexes **4**.

Upon collision-induced dissociation (Scheme 2), **XIII** and **XIII″** give analogous daughter ion spectra. Their common fragmentation pattern involves mainly the peroxidic ligand, so that ions at *m/z* = 270 and 228 (ions **XIV** and **XIV″**, respectively) are produced from the cleavage of the *t*-Bu−O bond and peaks at *m/z* = 254 (**VI**) and 212 (**VI″**) derive from the peroxidic O−O bond scission. Moreover, the monomeric nature of the peroxometal complex accounts for the previously discussed results obtained in the asymmetric oxidation of the model substrate benzyl *p*-tolyl sulfide, which show no contribution from crossed-type Ti(IV)/**1** active oxidants, displaying more than one molecule of the trialkanolamine ligand in the coordination sphere of the metal.

(37) The achiral peroxo complex **4c** is unstable at 21 °C and decomposes readily in the presence of an excess of TBHP.

Table 7. Energies (Hartrees) and Selected Bond Distances (Å) of Peroxidic Complex **4a** and of Isomers **A**−**D** of Ion **XIII** Calculated at the RHF/3-21G(*) Theoretical Level

	4a	A	B	C	D
energies					
in Hartrees	−1776.103 077	−1776.445 272	−1776.471 126	−1776.483 918	−1776.492 499
in kcal/mol		+24.9	+13.3	+5.3	0.00
		Bond Distances			
Ti−O(1)	1.82	1.78	1.77	1.77	1.81
Ti−O(2)	1.81	1.77	1.79	1.77	1.79
Ti−O(3)	1.79	1.82	1.78	1.78	1.82
Ti−O(4)	1.91	1.90	2.01	2.05	1.91
Ti−O(5)	2.10	2.00	2.57	2.72	2.10
Ti−N	2.48	3.43	2.27	2.25	2.48
O(4)−O(5)	1.50	1.50	1.51	1.48	1.50
O(5)−C(1)	1.48	1.50	1.58	1.53	1.48

Scheme 2. MS^2 Fragment Ions after CID of Peroxidic Ions **XIII** (m/z = 326) and **XIII″** (m/z = 284)
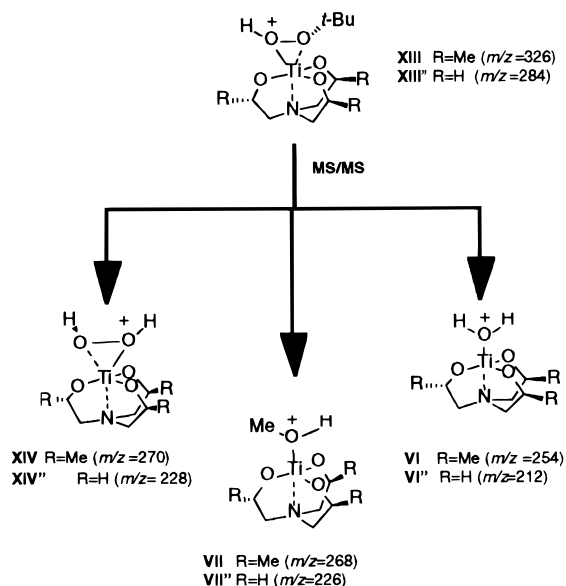
Concerning the structural assignment of ion **XIII,** ab initio calculations (RHF/3-21G(*)) have been performed to gain insight about the favored protonation site in peroxo complex **4a**. In Table 7, energies obtained for the neutral complex (*S,S,S*)-**4a** and for the different isomers of ion **XIII** are reported.[38,39] These latter derive from protonation at the four possible basic sites of the molecule namely: the two peroxygen atoms (structures **A** and **B**), the equatorial alkoxy functionality, and the tertiary nitrogen atom of the coordinated trialkanolamine ligand (structures **C** and **D**, respectively).

According to the theoretical calculations, structure **D** is highly destabilized, as the *N*-protonated ligand loses its tetracoordination to the titanium center (cf. Ti−N bond distance in **4a** and in **D**, Table 7). To the contrary, protonation at the equatorial trialkoxyamine oxygen affords the most stable isomer **C** and a minor reorganization of the geometry of the complex. Because

of the small energy difference, the protonated isomers **A**, **B**, and **C** are all likely to be present.[40]

Conclusions

In this work, the solution structure of chiral Ti(IV)/trialkanolamine complexes has been elucidated throughout the combined use of ESI-MS and ¹H NMR techniques.

The main results, which have provided a definite picture of the catalytic system under examination, can be summarized as follows:

(a) The catalyst structure depends on the Ti(IV)/ligand **1** stoichiometric ratio. When a 1:1 ratio is used, monomeric, highly symmetric complexes are obtained. An excess of ligand **1** induces the production of polynuclear Ti(IV) species, whose architecture is organized by a central molecule of trialkanolamine **1** with one, two, or three chiral titanatrane units appended. In such complexes, the apical ligand is too labile and only partially survives the electrospray ionization conditions. Therefore, ESI-MS analysis does not allow the determination of the thermodynamic distribution of the different Ti(IV) species equilibrating in solution.

(b) Fast ligand exchange equilibria occur in solution among the Ti(IV) complexes. In fact, both via ESI-MS and ¹H NMR, crossed-type Ti(IV)/**1a,b** adducts were detected in the presence of both ligands. Nevertheless, kinetic experiments dealing with the stereoselective sulfoxidation catalyzed by the scrambled complexes point out the independent reactivity of the two enantiopure catalysts.

(c) The key observation is that the active Ti(IV) peroxo complexes **4**, obtained both from the monomeric **2** and from the polynuclear aggregates **3** in the presence of an excess of TBHP, are themselves monomeric.

Taken as a whole, the present study has evidenced the important role played by the tetradentate ligands **1** in stabilizing Ti(IV) catalytic precursors and active species. It should be pointed out that the Ti(IV)/**1** sulfoxidation system is remarkably robust, reaching up to 1000 turnovers.[41] The fact that the highly reactive peroxo complexes **4** survive the conditions of ESI-MS bodes well for the extension of this approach to the study of other metal-mediated processes[42]

(38) The calculated geometrical parameters for peroxide **4a** are comparable with previously reported data for Ti(IV) trialkanolamine complexes from difrattometric analysis (see refs 24 and 25) and calculations performed on other monomeric transition metal peroxides; see: (a) Bonchio, M.; Di Furia, F.; Licini, G.; Modena, G.; Moro, S.; Nugent, W. A. *J. Am. Chem. Soc.* **1997**, *119*, 6935. (b) Wu, Y.-D.; Lai, D. K. W. *J. Am. Chem. Soc.* **1995**, *117*, 11327. (c) Wu, Y.-D.; Lai, D. K. W. *J. Org. Chem.* **1995**, *60*, 673. (d) Jørgensen, K. A. *J. Chem. Soc., Perkin Trans. 2* **1994**, 117. (e) Boche, G.; Bosold, F.; Lohrenz, J. C. W. *Angew. Chem., Int. Ed. Engl.* **1994**, *33*, 1161.

(39) The optimized geometries of complex (*S,S,S*)-**4a** and of the isomers **A**−**D** of ion **XIII** are reported in the Supporting Information, Figure S2.

(40) Worthy of notice is that protonation at the peroxidic ligand causes the loosening of its η^2 coordination geometry, thus indicating that both forms **A** and **B** could afford the fragmentation pattern observed in the MS^2 experiments. Indeed, elongation of the O−*t*-Bu bond occurring in **B** could explain the loss of the isobutene residue hypothesized in Figure 11.

(41) Bonchio, M.; Licini, G. Unpublished results.

(42) For a direct proof of reactive manganese(V) oxo species, see: Feichtinger, D.; Plattner, D. A. *Angew. Chem., Int. Ed. Engl.* **1997**, *36*, 1718.

Experimental Section

General Methods. ^{1}H NMR spectra were recorded on a Bruker AC-200 SY (200 MHz) or an AC-250 (250 MHz) instrument. Gas chromatographic analyses were performed using a Hewlett-Packard 5890 series II GC equipped with an SE-30 15-m × 0.25-mm-i.d. capillary column, using 4-methyl benzophenone as internal standard. Benzyl *p*-tolyl sulfoxide enantiomeric excesses and absolute configuration were determined directly on reaction mixtures by HPLC analysis performed on a Water Associates HPLC/GPC (FDP) 201 pump and a Water Associates 440 UV detector (λ = 254 nm) with a Lichrosorb S100 (*S,S*)-CSP-DACH-DNB [(250 × 4.0 mm i.d.] chiral column[43,44] (*n*-hexane/2-propanol (8:2) as eluent, flow rate of 2.0 mL/min, *P* = 1000 psi) according to the elution order [the (*S*) enantiomer is eluted before the (*R*) one]. Yields and product distributions were determined via quantitative GC analysis. Benzyl *p*-tolyl sulfide and sulfoxide spectral data match those already reported.[45] ESI-MS experiments were performed with a Finnigan LCQ instrument, with an upper mass limit of $m/z \approx 1850$, through direct infusion via a syringe pump. Standard experimental conditions were as follow: sample concentration, 10^{-3}M; flow rate, 8 μL min^{-1}; nebulizing gas, N$_2$ (40 units flow rate); spray voltage, 4 kV; capillary voltage, 25 V; capillary temperature, 120 °C; tube lenses offset, 30 V. The parameters related to octapoles and detector were those achieved by the automatic setup procedure. Collision-induced decompositions of selected ions were obtained by applying a supplementary radio frequency voltage (tickling voltage) to the end-cap electrodes of the ion trap (resonance activation). In the experiments aimed at the detection of peroxometal species, the capillary temperature was set at 80 °C. Cs$^+$ fast ion bombardment (FIB$^+$) mass spectra have been collected on a multiple quadrupole instrument (VGQuattro, VGBiotech, Altrincham, UK). The cesium ion gun was operated at an accelerating voltage of 15 kV and a heating current of 2.4 A. Test samples were prepared by dissolving the investigated precursor (0.1 mg) in 3-nitrobenzyl alcohol (NBA) used as the liquid matrix. Electron impact (EI) mass experiments have been performed on a VG AUTOSPEC instrument operating at 70 eV.

Computational Study. Ab initio calculations were carried out with the program systems Spartan v.4[46] and Gaussian 94,[47] running on IBM RS/6000 workstations. The molecular geometries were optimized using the 3-21G(*) basis set at the Hartree−Fock (HF) level of theory.

Chemicals. HPLC grade solvents were generally used. Methanol-d_4 (Fluka) and water-^{18}O, 20%, (C.I.L.) were used in the labeling experiments. Dichloromethane was distilled over CaH$_2$ and stored over molecular sieves. 1,2-Dichloroethane (DCE) was washed 3 times with 10% concentrated H$_2$SO$_4$ and with water several times to a pH of 7, dried over CaCl$_2$ overnight, distilled over P$_2$O$_5$, and stored over molecular sieves. *tert*-Butyl hydroperoxide (Fluka, 80%, 20% di-*tert*-butylperoxide) was purified by distillation under vacuum (bp 31−32 °C/16 Torr) and stored at 0 °C. Cumyl hydroperoxide (80% in cumene, Fluka) was stored over molecular sieves at 0 °C. Titanium(IV) tetraisopropoxide (Aldrich) was distilled under vacuum (bp 60−63 °C/0.1 Torr). Benzyl *p*-tolyl sulfide was prepared by alkylation of sodium *p*-tolylthiolate.[48] Enantiopure trialkanolamines **1a,b** were prepared following the literature procedure.[24] Triethanolamine (Aldrich) was distilled under reduced pressure (bp 190−193 °C/5 Torr).

Ti(IV)/1 in Situ-Formed System (Catalyst 2). A 0.025 M solution of catalyst **2** in CHCl$_3$ or CDCl$_3$ was prepared in a 2-mL volumetric flask by mixing 0.500 mL of a mother solution of ligand **1** (0.100 M) in the same solvent with a stoichiometric amounts of Ti(*i*-PrO)$_4$ (0.015 mL, 0.05 mmol). For performing the ESI-MS experiments, the mother solution of catalyst **2** was diluted by a factor of 10. Solutions of catalyst **2** containing increasing amount of ligand **1** (Figures 1 and 2) were prepared by appropriate dilutions of the starting ligand **1** mother solution.

Ti(IV)/1 *Preformed* System (Catalyst 3). Ti(O-*i*-Pr)$_4$ (0.1 mL, 0.33 mmol) was added to a solution of ligand **1** (0.44 mmol) in anhydrous CH$_2$Cl$_2$ (5 mL) under a nitrogen atmosphere. After the solution was stirred for 5 min at room temperature, the solvent was removed under reduced pressure. The recovered material was twice dissolved in dichloromethane (2 × 5 mL), and the solvent was removed again under vacuum. After the material was washed with hexane (6 mL), the solvent was removed under vacuum, yielding a white solid that was dried under high vacuum (0.1 mmHg) for 1 h and stored under nitrogen.

Procedure for the Kinetic Study of the Stereoselective Oxidation of Benzyl *p*-Tolyl Sulfide. A typical procedure is the following: in a 10-mL volumetric flask, Ti(*i*-PrO)$_4$ (0.015 mL, 0.05 mmol), ligand **1** (0.05 mmol), and benzyl *p*-tolyl sulfide (1.164 g, 5.440 mmol) were dissolved in dry DCE. After the mixture was cooled to −20 °C, cumyl hydroperoxide (0.100 mL, 0.544 mmol) was added under magnetic stirring. At the reaction times stated in Figure 10, a sample of the mixture (0.025 mL) was taken out and immediately quenched with an excess of di-*n*-butyl sulfide for the determination of conversion and product distribution (GC analysis), and for the ee and absolute configuration determination of benzyl *p*-tolyl sulfoxide (HPLC analysis). The asymmetric oxidation performed in the presence of the mixed catalytic system (**2a** + **2b**) was performed by introducing both ligand **1a** (0.025 mmol) and ligand **1b** (0.025 mmol) in the reaction mixture.

Labeling Experiments Performed by ESI-MS. The experiment aimed at the detection of ion **I** (^{18}O) was run by injecting into the mass spectrometer a methanol solution of catalyst **3a** (2 mL), in the presence of H$_2$^{18}O (20%, 20 μL added to the mobile phase). ^{18}O incorporation can be calculated from the two isotopic clusters collected for ion **I** before and after the labeling of the mobile phase according to the following formula: %[^{18}O$_{inc}$] = [%(M + 2)$_{^{18}O}$ − %(M + 2)$_{^{16}O}$]/%M$_{^{18}O}$ + [%(M + 2)$_{^{18}O}$ − %(M + 2)$_{^{16}O}$]. Based on the experimental isotopic distributions, the following isotopic distributions (ID) are found: for **I**(^{16}O), ID (exp %, calc %) = 722 (19, 31); 723 (25, 39); 724 (100, 100); 725 (50, 53); 726 (28, 33); 727 (7, 11); for **I**(^{18}O), ID (exp %) = 722 (19); 723 (25); 724 (100); 725 (48); 726 (43); 727 (14), 728 (8). Considering the actual ^{18}O content of the labeled water used (20%), we calculated that [^{18}O$_{inc}$] ≥ 65% (the diluition of the H$_2$O^{18} with unlabeled water present in the mobile phase was not considered in the former calculation).

Detection of Peroxometal Complexes 4a and 4c by ESI-MS. For these experiments, a solution of catalyst **3** in methanol or chloroform (2 mL) containing TBHP (200 μL) was injected into the ESI-MS instrument. The resulting spectra showed a significant reduction of the signals relative to the polynuclear Ti(IV) species and the appearance of a new peak in the monomeric region as follows: for ion **XIII**, ID (exp %, calc %) = 324 (12, 11); 325 (19, 12); 326 (100, 100); 327 (22, 23); 328 (9, 10); MS^2 = 270 (M$^+$ − C$_4$H$_8$), 254 (M$^+$ − C$_4$H$_8$O), 268 (ion **VII**);[49] for ion **XIII''**, ID (exp %, calc %) = 282 (10, 11); 283 (10, 11); 284 (100, 100); 285 (19, 19); 286 (10, 10); MS^2 = 228 (M$^+$ − C$_4$H$_8$), 212 (M$^+$ − C$_4$H$_8$O), 226 (ion **VII''**).[49]

ESI-MS Isotopic Distributions and MS^2 Data for Selected Ions Not Reported in the Body of the Paper: for **VIII**, ID (exp %, calc %) = 487 (20, 21); 488 (25, 24); 489 (100, 100); 490 (37, 36); 491 (20, 20); MS^2 (%) = 445 (M$^+$ − CH$_3$CHO); for **IX**, ID (exp %, calc %) = 501 (19, 21); 502 (22, 25); 503 (100, 100); 504 (33, 37); 505 (19, 20); MS^2 = 459 (M$^+$ − CH$_3$CHO). When perdeuterated methanol was used as the mobile phase, the isotopic cluster of ion **IX** showed an increment of 3 mass units consistent with the formula C$_{19}$H$_{36}$D$_3$O$_7$N$_2$-

(43) Gargano, G.; Gasparrini, F.; Misiti, D.; Palmieri, G.; Pierini, M.; Villani, C. *Chromatographia* **1987**, *24*, 505.

(44) Altomare, C.; Carotti, A.; Cellamare, S.; Fanelli, F.; Gasparrini, F.; Villani, C.; Carrupt, P.-A.; Testa, B. *Chirality* **1993**, *5*, 527.

(45) Lonoshita, M.; Sato, Y.; Kunieda, N. *Chem. Lett.* **1974**, 377.

(46) *Spartan* v.4.0, Wavefunction, Inc., 18401 von Karman Ave. #370, Irvine, CA 92715, 1995.

(47) Frisch, M. J.; Trucks, G. W.; Schlegel, H. B.; Gill, P. M. W.; Johnson, B. G.; Robb, M. A.; Cheeseman, J. R.; Keith, T.; Petersson, G. A.; Montgomery, J. A.; Raghavachari, K.; Al-Laham, M. A.; Zakrzewski, V. G.; Oritz, J. V.; Foresman, J. B.; Cioslowski, J.; Stefanov, B. B.; Nanayakkara, A.; Challacombe, M.; Peng, C. Y.; Ayala, P. Y.; Chen, W.; Wong, M. W.; Andres, J. L.; Replogle, E. S.; Gomperts, R.; Martin, R. L.; Fox, D. J.; Binkley, J. S.; Defrees, D.; Baker, J. J.; Steward, J. P.; Head-Gordon, M.; Gonzales, C.; Pople, J. A. *Gaussian 94*, Revision C.2; Gaussian Inc.: Pittsburgh, PA, 1995.

(48) Peach, M. E. In *The Chemistry of Thiol Group*, Patai, S., Ed.; John Wiley and Sons, Ltd.: Bristol, 1974; Part 2, pp 721−784.

(49) Ion likely originating from the reaction of ion **X** with neutral solvent molecules (methanol) (see also ref 33).

Ti_2 as follows: **IX**(D_3), ID (exp %, calc %) = 504 (27, 21); 505 (23, 25); 506 (100, 100); 507 (29, 37); 508 (16, 21); MS^2 = 462 (M^+ − CH_3CHO).

FIB$^+$-MS Isotopic Distributions and MS^2 Data for Selected Ions Not Given in the Body of the Paper: for ion **X**, ID (exp %, calc %) = 234 (16, 11); 235 (15, 11); 236 (100, 100); 237 (21, 18); 238 (12, 9); MS^2 = 205 (M^+ − CH_3O), 192 (M^+ − CH_3CHO).

Supporting Information Available: ^{1}H NMR spectra in deuteriochloroform of ligands **1a** and **1b**, ligands **1a** (2.5×10^{-2} M) and **1b** (2.5×10^{-2} M) + Ti(i-PrO)$_4$, complex **2a** + **1b**, complex **2a**, and complex **2b**; ab initio [RHF/3-21G(*)] optimized structures and energies (Hartrees) of peroxo complex **4a** and of isomers of ion **XIII**; and ^{1}H NMR of peroxo complexes **4** (PDF). This material is available free of charge via the Internet at http://pubs.acs.org.